航空技術學院學報　第十四卷　第一期　第 19－34 頁（民國一〇四年）
Journal of Air Force Institute of Technology, Vol. 14, No. 1, pp. 19-34, 2015

Temperature-Dependent Viscosity and Uniform Blowing/Suction Effects on Combined Heat and Mass Transfer by Natural Convection about the Vertical Cylinder in Porous Media

飽和多孔性介質內隨溫度變化之黏度與均勻噴吸流效應對於流經一垂直圓柱體自然對流熱傳與質傳影響

Kuo-Ann Yih, Chuo-Jeng Huang
易國安、黃卓礽
Department of Aircraft Engineering, Air Force Institute of Technology
飛機工程系，空軍航空技術學院

Abstract

The temperature-dependent viscosity and uniform blowing/suction effects on combined heat and mass transfer by the natural convection about the vertical cylinder embedded in a saturated porous medium are numerically analyzed. The viscosity of the fluid varies inversely as a linear function of the temperature. The surface of the vertical cylinder is maintained at linear wall temperature and liner wall concentration (LWT/LWC). The transformed governing equations are the similarity solution and solved by Keller box method (KBM). Numerical data for the dimensionless temperature profile, the dimensionless concentration profile, the local Nusselt number and the local Sherwood number are presented for the viscosity-variation parameter θ_e, the buoyancy ratio N, the Lewis number Le, the transverse curvature parameter ξ and the blowing/suction parameter f_w. In general, for the case of suction ($f_w > 0$), increases the local heat transfer rate as well as the local mass transfer rate between the surface and the porous medium. This trend reversed for the case of blowing ($f_w < 0$). The local Nusselt number as well as the local Sherwood number increases with increasing the transverse curvature parameter ξ and the buoyancy ratio N. For a given positive N (negative N), as the Lewis number increases, the local Nusselt number decreases (increases). While, for a given N, as the Lewis number increases, the local Sherwood number always increases. It is also found that for $\theta_e < 0$ (liquid), both the local Nusselt number and the local Sherwood number are greater than the constant viscosity ($\theta_e \to \infty$) cases, while, these are less for $\theta_e > 0$ (gas).

Keywords: temperature-dependent viscosity, uniform blowing/suction effect, heat and mass transfer by natural convection, vertical cylinder, saturated porous media

摘　要

本文以一數值方法來分析：隨溫度變化之黏度與均勻噴/吸流效應對於飽和多孔性介質內垂直圓柱體自然對流熱與質量傳遞之影響。流體的黏度隨溫度的線性函數而成反比。垂直圓柱體的表面維持於線性壁溫度/線性壁濃度。吾人以凱勒盒子法來解轉換過的控制方程式。數

值計算結果主要顯示：黏度變化參數，浮力比，路易士數，橫向曲率參數，噴/吸流參數，對無因次溫度分佈、無因次濃度分佈、局部紐塞爾數和局部希爾吾德數之影響。一般而言，局部表面熱與質量傳遞率均因吸入流效應（噴/吸流參數為正值）而增加。反之，對噴出流效應（噴/吸流參數為負值）則減少。局部紐塞爾數和局部希爾吾德數均會隨著橫向曲率參數與浮力比的增加而增大。對於正值（負值）浮力比的情況，當路易士數增加時，局部紐塞爾數會隨之減小（增大）。然而，當路易士數增加時，局部希爾吾德數仍會隨之增大。當黏度變化參數為負值時（液體），則局部紐塞爾數和局部希爾吾德數均會大於均勻黏度（黏度變化參數趨近於無窮大）之數值。相反地，當黏度變化參數為正值時（液體），則為相反情況：局部紐塞爾數和局部希爾吾德數均會小於均勻黏度之數值。

關鍵字：隨溫度變化之黏度，均勻噴/吸流效應，熱與質傳自然對流，垂直圓柱體，飽和多孔性介質

1. Introduction

Coupled heat and mass transfer (or double-diffusion) driven by buoyancy, due to temperature and concentration variations in a saturated porous medium, has several important applications in geothermal and geophysical engineering, for example, the migration of moisture in fibrous insulation and the underground disposal of nuclear wastes. Recent books by Nield and Bejan [1], Vafai [2] and Ingham and Pop [3] present a comprehensive account of the available information in the field.

In the aspect of pure heat transfer, Minkowycz and Cheng [4] adopted the local non-similarity solution to analyze the free convection about a vertical cylinder embedded in a porous medium (VWT: variable wall temperature). Kumari et al. [5] used the finite-difference and improved perturbation solution to study free convection on a vertical cylinder embedded in a saturated porous medium. Free convection from a vertical cylinder embedded in a saturated porous medium was presented by Merkin [6] (series method) and Bassom and Rees [7] (asymptotic solution and Keller Box method). The influence of injection or withdrawal of fluid on free convection about a vertical cylinder (UWT: uniform wall temperature) in a porous medium was also investigated by Yücel [8] and Huang and Chen [9] using Keller Box method.

In the aspect of coupled heat and mass transfer, Lai et al. [10] studied the coupled heat and mass transfer by natural convection from slender bodies of revolution in porous media. Yücel [11] investigated the natural convection heat and mass transfer along a vertical cylinder in a porous medium. Integral treatment of coupled heat and mass transfer by natural convection from a cylinder in porous media was presented by Singh and Chandarki [12]. Cheng [13] numerically studied the double diffusion from a horizontal cylinder of elliptic cross section with uniform wall heat and mass fluxes (UHF/UMF) in a porous medium.

In all of the above mentioned studies the viscosity of the fluid was assumed to be constant. However it is known that this physical property may change significantly with the temperature of the fluid. The temperature-dependent fluid viscosity is important when the temperature gradients and concentration gradients are high. Thus in order to predict the fluid flow behavior accurately it is necessary to consider the variation of the viscosity.

In the aspect of pure heat transfer in the porous medium, Gary et al. [14] studied the effects of significant viscosity variation on convective heat transfer transport in water-saturated porous medium. Lai and Kulacki [15] presented the effect of variable viscosity on convective heat transfer along a vertical surface (UWT) in a saturated porous medium. Kumari [16] investigated the variable viscosity effects on free and mixed convection boundary-layer flow from a horizontal surface in a saturated porous medium- variable heat flux (VHF). Vajravelu et al. [17] examined free convection boundary layer flow past a vertical surface in a porous medium with temperature-dependent properties.

Recently, in the aspect of coupled heat and mass transfer in a porous medium, Cheng [18] studied the non-similar boundary layer analysis of double-diffusive convection from a vertical truncated cone (UWT/UWC) in a porous medium with variable viscosity. Mahdy [19] extended the work of Cheng [18] to investigate the effect of chemical reaction and heat generation or absorption on double-diffusive convection from a vertical truncated cone in porous media with variable viscosity. Mahdy et al. [20] studied the double-diffusive convection with variable viscosity from a vertical truncated cone in porous media in the presence of magnetic field and radiation effects. Hassanien and Rashed [21] presented the non-Darcy free convection flow over a horizontal cylinder in a saturated porous medium with variable viscosity, thermal conductivity and mass diffusivity.

The objective of the present work, therefore, is to investigate numerically the temperature-dependent viscosity and uniform blowing/suction effects on the coupled heat and mass transfer by natural convection flow over a vertical cylinder subjected to linear wall temperature and linear wall concentration (LWT/LWC) embedded in porous media. It is assumed that the viscosity of the fluid is an inverse linear function of temperature. The governing equations have been solved numerically using Keller box method (KBM). The results are obtained for various values of the parameters.

2. Analysis

Let us consider the problem of the temperature-dependent viscosity and uniform blowing/suction effects on combined heat and mass free convection flow over a vertical cylinder embedded in a saturated porous medium. In order to obtain the similar solution, we consider the boundary condition of linear wall temperature $T_w(x)$ and linear wall concentration $C_w(x)$ (LWT/LWC), and V_w is the uniform blowing/suction velocity. $T_w(x)$ and $C_w(x)$ are higher than the ambient temperature T_∞ and concentration C_∞, respectively. Figure 1 shows the flow model and physical coordinate system. The origin of the coordinate system is placed at the leading edge of the vertical cylinder, where x and r are Cartesian coordinates measuring distance along and normal to the surface of vertical cylinder, respectively.

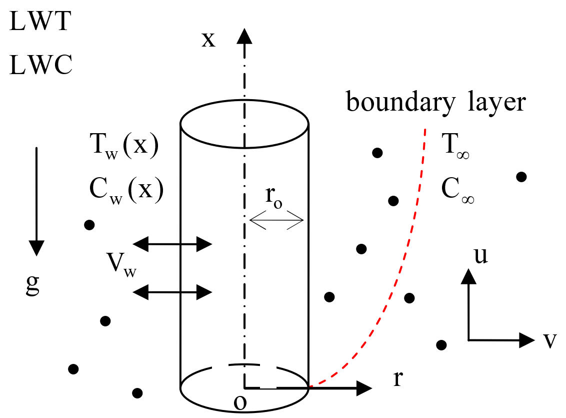

Fig. 1. The flow model and the physical coordinate system

All the fluid properties are assumed to be constant, except for the viscosity of fluid μ and except for the density variation in the buoyancy term. The viscosity of the fluid-saturated porous medium depends on the temperature T in the following form (see Lai and Kulacki [15]):

$$\frac{1}{\mu}=\frac{1}{\mu_\infty}\left[1+\gamma(T-T_\infty)\right]=a(T-T_e). \qquad (1)$$

where γ is a viscosity-variation constant and μ_∞ is the viscosity of the ambient fluid with the following relation

$$a=\frac{\gamma}{\mu_\infty} \text{ and } T_e=T_\infty-\frac{1}{\gamma}. \qquad (2)$$

Both a and T_e are constant and their values depend on the reference state and the thermal property of the fluid, i.e., γ. In general, $a > 0$ ($\gamma > 0$) for liquid and $a < 0$ ($\gamma < 0$) for gas. The viscosity of the fluid usually reduces with increasing temperature while it enhances for gas.

Introducing the boundary layer and Boussinesq approximations, the governing equations and the boundary conditions based on the Darcy law (It is valid under the condition of low velocity and small pores of porous medium [22]) can be written as follows:

$$\frac{\partial(ru)}{\partial x}+\frac{\partial(rv)}{\partial r}=0, \qquad (3)$$

$$u=-\frac{K}{\mu}\left(\frac{\partial p}{\partial x}+\rho g\right), \qquad (4)$$

$$v=-\frac{K}{\mu}\left(\frac{\partial p}{\partial r}\right), \qquad (5)$$

$$u\frac{\partial T}{\partial x}+v\frac{\partial T}{\partial r}=\frac{\alpha}{r}\frac{\partial}{\partial r}\left(r\frac{\partial T}{\partial r}\right), \qquad (6)$$

$$u\frac{\partial C}{\partial x}+v\frac{\partial C}{\partial r}=\frac{D_M}{r}\frac{\partial}{\partial r}\left(r\frac{\partial C}{\partial r}\right), \qquad (7)$$

$$\rho=\rho_\infty\left[1-\beta_T(T-T_\infty)-\beta_C(C-C_\infty)\right], \qquad (8)$$

$$r=r_o:\ v=V_w,\ T=T_w(x)=T_\infty+a_1x,\ C=C_w(x)=C_\infty+b_1x, \qquad (9.1\text{-}3)$$

$$r\to\infty:\ u=0,\ T=T_\infty,\ C=C_\infty. \qquad (10.1\text{-}3)$$

Here, u and v are the Darcian velocities in the x- and r- directions; K is the permeability of the porous medium; p and ρ are the pressure and the density of the fluid, respectively; g is the gravitational acceleration; T and C are the volume-averaged temperature and concentration, respectively; α and D_M are the equivalent thermal diffusivity and mass diffusivity, respectively; β_T and β_C are the thermal and concentration expansion coefficients of the fluid, respectively; r_o is the radius of the vertical cylinder; a_1 and b_1 are positive constants.

The stream function ψ is defined by

$$ru=\partial\psi/\partial r,\quad rv=-\partial\psi/\partial x. \qquad (11)$$

Therefore, the continuity equation is automatically satisfied.

We now pay attention to governing equations

(4) and (5). If we do the operation of the cross-differentiation $\partial(\mu\ u)/\partial r - \partial(\mu\ v)/\partial x$, then the pressure terms in equations (4) and (5) can be eliminated. Further, with the help of the equation (8) and the boundary layer approximation $(\partial/\partial x << \partial/\partial r)$, then we can obtain

$$\frac{\partial(\mu\ u)}{\partial r} = \rho_\infty g K\left(\beta_T \frac{\partial T}{\partial r} + \beta_C \frac{\partial C}{\partial r}\right). \quad (12)$$

Invoking the following dimensionless similarity variables:

$$\eta = \frac{r_o Ra_x^{1/2}}{2x}\left(\frac{r^2}{r_o^2} - 1\right) \quad (13.1)$$

$$f(\eta) = \frac{\psi}{\alpha r_o Ra_x^{1/2}} \quad (13.2)$$

$$\theta(\eta) = \frac{T - T_\infty}{T_w(x) - T_\infty} = \frac{T - T_\infty}{a_1 x} \quad (13.3)$$

$$\phi(\eta) = \frac{C - C_\infty}{C_w(x) - C_\infty} = \frac{C - C_\infty}{b_1 x} \quad (13.4)$$

$$Ra_x = \frac{\rho_\infty g \beta_T [T_w(x) - T_\infty] K x}{\mu_\infty \alpha} = \frac{\rho_\infty g \beta_T a_1 K x^2}{\mu_\infty \alpha} \quad (13.5)$$

Substituting equation (13) into equations (3), (12), (6)-(7), (9)-(10), we obtain

$$f' = \left(1 - \frac{\theta}{\theta_e}\right)(\theta + N\phi), \quad (14)$$

$$(1+\xi\eta)\theta'' + (\xi + f)\theta' - f'\theta = 0, \quad (15)$$

$$\frac{(1+\xi\eta)}{Le}\phi'' + \left(\frac{\xi}{Le} + f\right)\phi' - f'\phi = 0. \quad (16)$$

The boundary conditions are defined as follows:

$$\eta = 0:\ f = f_w,\ \theta = 1,\ \phi = 1, \quad (17)$$

$$\eta \to \infty:\quad \theta = 0,\ \phi = 0. \quad (18)$$

Equation (14) can be obtained by integrating equation (12) once and with the aid of boundary condition (10.1-3).

The transverse curvature parameter ξ is defined as below

$$\xi = \frac{2x}{r_o Ra_x^{1/2}}. \quad (19)$$

From equation (19), it is found that ξ is independent of x and allows the similarity

In addition, in terms of the new variables, the Darcian velocities in x- and r- directions are, respectively, given by

$$u = \frac{\alpha Ra_x}{x} f', \quad (20)$$

$$v = -\frac{\alpha Ra_x^{1/2}}{x}\frac{1}{(1+\xi\eta)^{1/2}} f, \quad (21)$$

where primes denote differentiation with respect to η.

Inserting equation (9.1) into equation (21), we can find that the blowing/suction parameter f_w is defined as followed

$$f_w = f(0) = -\frac{V_w x}{\alpha Ra_x^{1/2}} = \text{constant}. \quad (22)$$

On the one hand, for the case of blowing, $V_w > 0$ and hence $f_w < 0$. On the other hand, for the case of suction, $V_w < 0$ and hence $f_w > 0$.

With the help of equations (13.3) and (2), the viscosity-variation parameter θ_e is a constant and is defined by

$$\theta_e = \frac{T_e - T_\infty}{T_w(x) - T_\infty} = -\frac{1}{\gamma[T_w(x) - T_\infty]}. \quad (23)$$

Its value is determined by the viscosity of the fluid in considering and the operating temperature difference. On the one hand, a large value of θ_e implies either γ or $[T_w(x) - T_\infty]$ are small. From equation (1), it is worth mentioning that for $\gamma \to 0$, i.e., $\mu = \mu_\infty$ (constant viscosity) then $\theta_e \to \infty$. On the other hand, for a smaller value of θ_e, either the viscosity of the fluid changes apparently with temperature or the operating temperature difference is large. It is also important to note that θ_e is negative for liquid and positive for gas.

Besides, the buoyancy ratio N and the Lewis number Le are, respectively, defined as followed:

$$N = \frac{\beta_C(C_w - C_\infty)}{\beta_T(T_w - T_\infty)} = \frac{\beta_C b_1}{\beta_T a_1}, \qquad Le = \frac{\alpha}{D_M}. \quad (24)$$

The parameter N measures the relative importance of mass and thermal diffusion in the buoyancy-driven flow. It is apparent that N is zero for thermal-driven flow, positive for thermally assisting flow, negative for thermally opposing flow.

The results of practical interest in many applications are both the surface heat and mass transfer rates. The surface heat and mass transfer rates are expressed in terms of the local Nusselt number Nu_x and the local Sherwood number Sh_x respectively, which are basically defined as followed:

$$Nu_x = \frac{h_x x}{k} = \frac{q_w x}{[T_w(x) - T_\infty]\ k}. \quad (25)$$

$$Sh_x = \frac{h_{m,x} x}{D_M} = \frac{m_w x}{[C_w(x) - C_\infty]\ D_M}. \quad (26)$$

where h_x, $h_{m,x}$ are local convective heat transfer coefficient and local convective mass transfer coefficient, respectively; k is the equivalent thermal conductivity; q_w and m_w are the local heat flux and the local mass flux, respectively; and $q_w = h_x[T_w(x) - T_\infty]$ (the Newton's law of cooling) and $m_w = h_{m,x}[C_w(x) - C_\infty]$ (the analogy between the mass transfer and the heat transfer).

From the Fourier's law of heat conduction and the Fick's law of mass diffusion, the rate of heat transfer q_w and the rate of mass transfer m_w are respectively defined by:

$$q_w = -k\left(\frac{\partial T}{\partial r}\right)\bigg|_{r=r_o} \quad \text{and} \quad m_w = -D_M\left(\frac{\partial C}{\partial r}\right)\bigg|_{r=r_o}. \quad (27)$$

Inserting equation (27) into equations (25)-(26) and with the aid of equation (13), the local Nusselt number Nu_x and the local Sherwood number Sh_x in terms of $Ra_x^{1/2}$ are, respectively, obtained by

$$\frac{Nu_x}{Ra_x^{1/2}} = -\theta'(\xi,0). \quad (28)$$

$$\frac{Sh_x}{Ra_x^{1/2}} = -\phi'(\xi,0). \quad (29)$$

It may be noticed that for N = 0 (pure heat transfer), $\theta_e \to \infty$ (constant viscosity) and $f_w = 0$ (impermeable), equations (14)-(15), (17.1-2)-(18.1) are reduced to those of Minkowycz and Cheng [4] where a similar solution was obtained previously. (The boundary value problem for ϕ then becomes ill-posed and is of no physical significance). For the case of $\xi = 0$ (vertical plate), $f_w = 0$ and $\theta_e \to \infty$, equations (14)-(18) are reduced to those of Yih [23].

3. Numerical Method

The present analysis integrates the system of equations (14)-(18) by the implicit finite difference approximation together with the modified Keller box method of Cebeci and Bradshaw [24]. To begin with, the partial differential equations are first converted into a system of five first-order equations. Then these first-order equations are expressed in finite difference forms and solved along with their boundary conditions by an iterative scheme. This approach gives a better rate of convergence and reduces the numerical computational times.

Computations were carried out on a personal computer with the first step size $\Delta\eta_1$ = 0.01. The variable grid parameter is chosen 1.01 and the value of η_∞ = 100. The iterative procedure is stopped to give the final temperature and concentration distributions when the errors in computing the $|\theta'_w|$ and $|\phi'_w|$ in the next procedure become less than 10^{-5}.

4. Results and Discussion

In order to verify the accuracy of our present method, we have compared our results with those of Minkowycz and Cheng [4], and Yih [23]. Table 1 shows the comparison of the values of $-\theta'(0)$ for various values of ξ with N = 0, $f_w = 0$, $\theta_e \to \infty$. Tables 2 and 3 list the comparison of the values of $-\theta'(0)$ and $-\phi'(0)$ for various values of N and Le with $\xi = 0$, $f_w = 0$, $\theta_e \to \infty$, respectively. The comparisons in all the above cases are found to be in excellent agreement, as shown in Tables 1-3. Tables 4 and 5 show the values of $-\theta'(0)$ and $-\phi'(0)$ for the various values of N, Le, θ_e, ξ and f_w, respectively.

With the help of equations (1), (13.3), and (23) the variable viscosity μ can be rewritten in the following form

$$\mu = \frac{1}{\left(1 - \frac{\theta(\eta)}{\theta_e}\right)}\mu_\infty. \tag{30}$$

Since $\theta(\eta)$ varies from 0 (at the edge of the thermal boundary layer, $\eta \to \infty$) to 1 (at the surface, η = 0), the largest change in the fluid viscosity from its ambient value μ_∞, occurs at the surface, i.e., $\theta(0)$ = 1, where

$$\mu = \frac{1}{\left(1 - \frac{1}{\theta_e}\right)}\mu_\infty. \tag{31}$$

Therefore, we cannot take value of θ_e between 0 and 1, and that the constraints, θ_e > 1 for gas and θ_e < 0 for liquid.

Table 1 Comparison of the values of $-\theta'(0)$ for various values of ξ with N = 0, $f_w = 0$, $\theta_e \to \infty$

ξ	$-\theta'(0)$	
	Minkowycz and Cheng [4]	Present
0.0	—	1.0000
1.0	1.179	1.1778
2.0	1.345	1.3435
3.0	1.502	1.4998
4.0	1.654	1.6492
5.0	1.803	1.7931
6.0	1.952	1.9327
7.0	2.102	2.0686
8.0	2.253	2.2015
9.0	2.407	2.3317
10.0	2.564	2.4597

Table 2 Comparison of the values of $-\theta'(0)$ for various values of N and Le with $\xi = 0$, $f_w = 0$, $\theta_e \to \infty$

N	Le	$-\theta'(0)$	
		Yih [23]	Present
4	1	2.2361	2.2361
4	10	1.6010	1.6011
4	100	1.2162	1.2166
1	1	1.4142	1.4142
1	10	1.1967	1.1968
1	100	1.0725	1.0726
−0.5	1	0.7072	0.7071
−0.5	10	0.8680	0.8680
−0.5	100	0.9508	0.9507

Table 3 Comparison of the values of $-\phi'(0)$ for various values of N and Le with $\xi = 0$, $f_w = 0$, $\theta_e \to \infty$

N	Le	$-\phi'(0)$	
		Yih [23]	Present
4	1	2.2361	2.2361
4	10	7.3726	7.3723
4	100	23.5781	23.5666
1	1	1.4142	1.4142
1	10	4.9064	4.9061
1	100	15.9134	15.9045
−0.5	1	0.7072	0.7071
−0.5	10	2.9373	2.9371
−0.5	100	9.9642	9.9568

Table 4 The values of $-\theta'(0)$ for various values of N, Le, θ_e, ξ and f_w

N	Le	θ_e	ξ	f_w	$-\theta'(0)$
10	1	10	0	−1	2.7278
5	5	2	5	0	2.3966
1	10	−2	10	1	3.2527
10	1	−10	0	−1	2.9755
5	5	10	5	0	2.6670
1	10	2	10	1	2.8994
10	1	−2	0	−1	3.4216
5	5	10	5	0	2.6670
1	10	∞	10	1	3.0894

Table 5 The values of $-\phi'(0)$ for various values of N, Le, θ_e, ξ and f_w

N	Le	θ_e	ξ	f_w	$-\phi'(0)$
10	1	10	0	−1	2.7278
5	5	2	5	0	5.2388
1	10	−2	10	1	14.2248
10	1	−10	0	−1	2.9755
5	5	10	5	0	6.2902
1	10	2	10	1	12.2354
10	1	−2	0	−1	3.4216
5	5	10	5	0	6.2902
1	10	∞	10	1	13.2036

The numerical results are presented for the buoyancy ratio N ranging from -0.5 to 5, Lewis number Le ranging from 0.1 to 10, the viscosity-variation parameter θ_e ranging from -10 to -2 (liquid), 2 to 10 (gas), the blowing/suction parameter f_w ranging from -1 to 1, and the transverse curvature parameter ξ ranging from 0 to 10.

Figures 2 and 3 show the dimensionless temperature and concentration profiles for two values of the blowing/suction parameter f_w ($f_w = -1$, 1) and the transverse curvature parameter ξ (ξ= 0, 10) with N = 5, Le = 2, $\theta_e = -2$, respectively. From these two figures, it is found that not only the dimensionless temperature profile but also the dimensionless concentration profile decreases monotonically from the surface to the ambient. On the one hand, for the fixed value of ξ, both the dimensionless wall temperature gradient $[-\theta'(\xi,0)]$ and the dimensionless wall concentration gradient $[-\phi'(\xi,0)]$ increase for the case of suction ($f_w > 0$). However, this trend reversed for the case of blowing ($f_w < 0$). On the other hand, for the fixed value of f_w, the dimensionless wall temperature and concentration gradients increase with increasing the transverse curvature parameter ξ.

Figures 4 and 5 display the dimensionless temperature and concentration profiles for two values of the buoyancy ratio N (N = -0.5, 5) and the Lewis number Le (Le = 0.1, 10) with f_w = 1, ξ = 5, $\theta_e = -5$, respectively. For a fixed value of Le, both the thermal boundary layer thickness δ_T and concentration boundary layer thickness δ_C decrease as the buoyancy ratio N increases, as illustrated in Figs. 4 and 5. It is also observed that, for thermally assisting (opposing) flow, i.e., N > 0 (N < 0), increasing the Lewis number Le increases (decreases) the thermal boundary layer thickness, as depicted in Fig. 4. Whereas, for case of the fixed N, when the Lewis number Le increases from 0.1 to 10, the concentration boundary layer thickness decreases, as shown in Fig. 5.

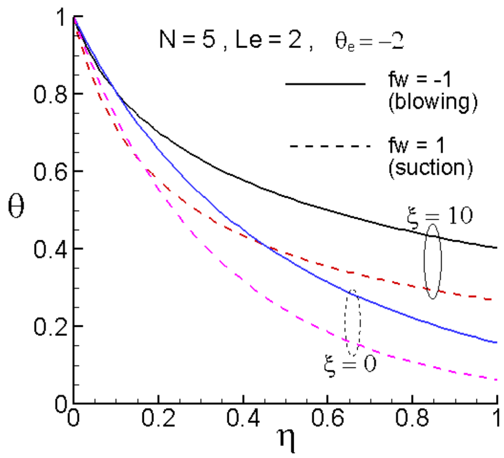

Fig. 2. Dimensionless temperature profile for two values of f_w and ξ

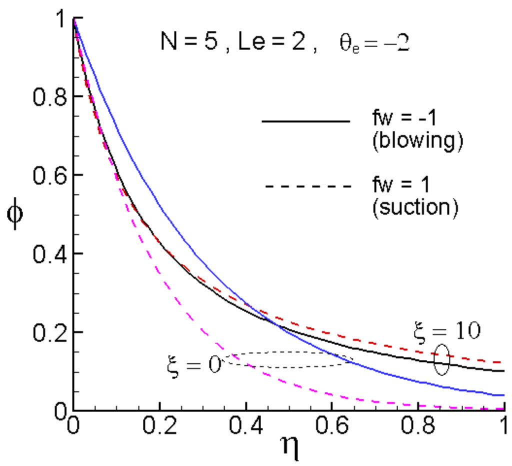

Fig. 3. Dimensionless concentration profile for two values of f_w and ξ

The dimensionless temperature and concentration profiles for three values of the viscosity-variation parameter θ_e ($\theta_e = 2, \infty$, and -2) with N = 1, Le = 5, $f_w = 0$, $\xi = 2$ are plotted in Figs. 6 and 7, respectively. The red dashed lines in both figures indicate the case of $\theta_e \to \infty$ (constant viscosity) in comparison with other values of θ_e corresponding to variable viscosity. It is observed that for $\theta_e > 0$ (gas), the effect of the viscosity-variation parameter leads to a tendency to thicken both the thermal boundary thickness and the concentration boundary thickness, thus decreases the dimensionless wall temperature gradient $[-\theta'(\xi,0)]$ and the dimensionless wall concentration gradient $[-\phi'(\xi,0)]$. While, they are suppressed for the case of $\theta_e < 0$ (liquid).

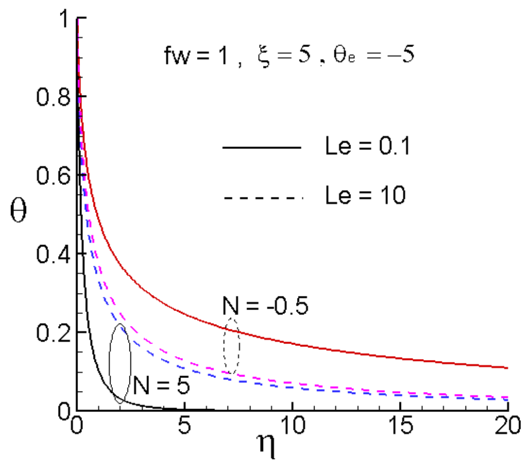

Fig. 4. Dimensionless temperature profile for two values of N and Le

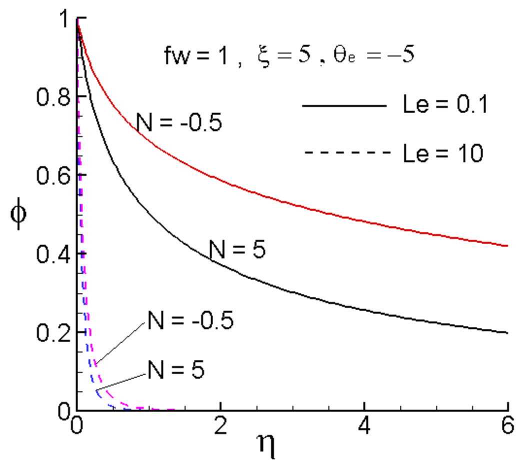

Fig. 5. Dimensionless concentration profile for two values of N and Le

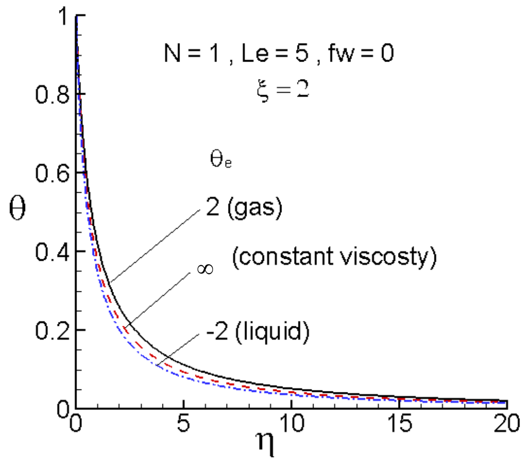

Fig. 6. Dimensionless temperature profile for three values of the viscosity-variation parameter

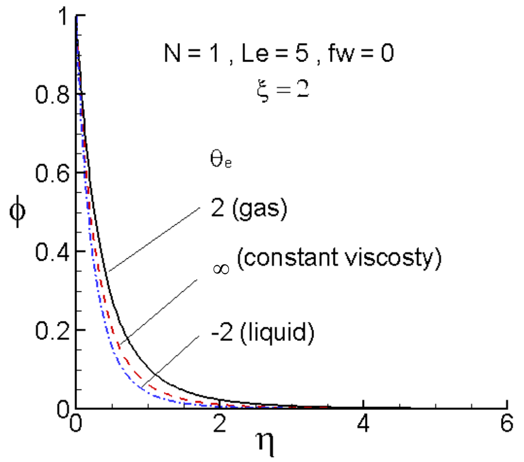

Fig. 7. Dimensionless concentration profile for three values of the viscosity-variation parameter

Figures 8 and 9 show the local Nusselt number $Nu_x / Ra_x^{1/2}$ and the local Sherwood number $Sh_x / Ra_x^{1/2}$ as functions of the blowing/suction parameter f_w for four values of the transverse curvature parameter ξ (ξ = 0, 1, 5, 10) with N = 5, Le = 2, $\theta_e = -2$, respectively. In general, for the fixed value of ξ, it has been found that both the local Nusselt number and the local Sherwood number increase due to the case of suction, i.e., f_w > 0. For the fixed value of f_w, enhancing the transverse curvature parameter ξ increases the local Nusselt number as well as the local Sherwood number. This is because for the case of suction (f_w > 0) and the larger transverse curvature parameter ξ will tend to increase the dimensionless wall temperature gradient as well as the dimensionless wall concentration gradient, as depicted in Figs. 2 and 3. From equations (28)-(29), the greater the dimensionless wall temperature and concentration gradients, the larger the local Nusselt number and the local Sherwood number. This trend reversed for the case of blowing (f_w < 0).

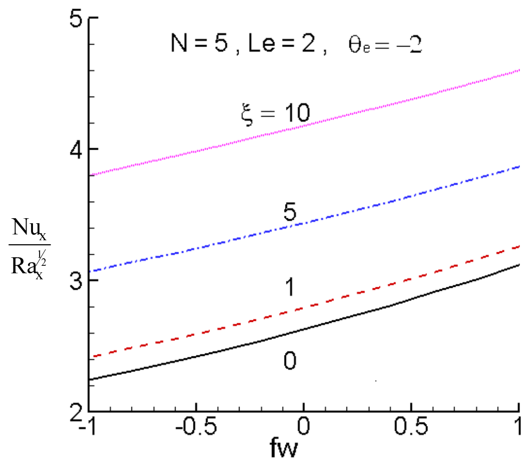

Fig. 8. Effect of the transverse curvature parameter on the local Nusselt number

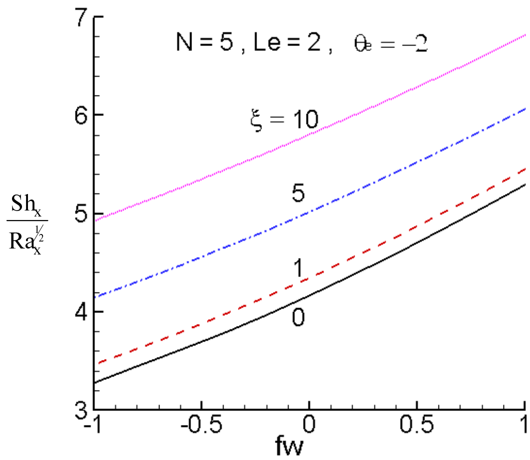

Fig. 9. Effect of the transverse curvature parameter on the local Sherwood number

The local Nusselt number $Nu_x / Ra_x^{1/2}$ and the local Sherwood number $Sh_x / Ra_x^{1/2}$ as functions of the blowing/suction parameter f_w for two values of the buoyancy ratio N (N = -0.5, 5) and the Lewis number Le (Le = 0.1, 10) with ξ = 5, $\theta_e = -5$ are illustrated in Figs. 10 and 11, respectively. On the one hand, for a fixed value of Le, increasing the buoyancy ratio N enhances both the local Nusselt number and the local Sherwood number. This is because the increase in the value of N reduces the thermal boundary layer thickness and the concentration boundary layer thickness, as shown in Figs. 4 and 5.

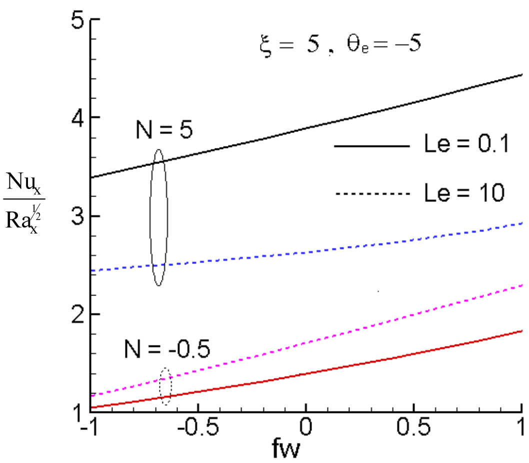

Fig. 10. Effect of the buoyancy ratio and the Lewis number on the local Nusselt number

On the other hand, for a given positive N, as the Lewis number increases from 0.1 to 10, the local Nusselt number decreases. This is due to the fact that a larger Lewis number Le is associated with a thicker thermal boundary layer thickness, as shown in Fig. 4. The thicker the thermal boundary layer thickness, the smaller the local Nusselt number. While, for a given negative N, as the Lewis number increases from 0.1 to 10, the local Nusselt number increases. For a given N, as the Lewis number increases from 0.1 to 10, the local Sherwood number increases. This is because that a larger Lewis number Le is associated with a thinner concentration boundary layer thickness, as shown in Fig. 5. The thinner the concentration boundary layer thickness, the greater the local Sherwood number.

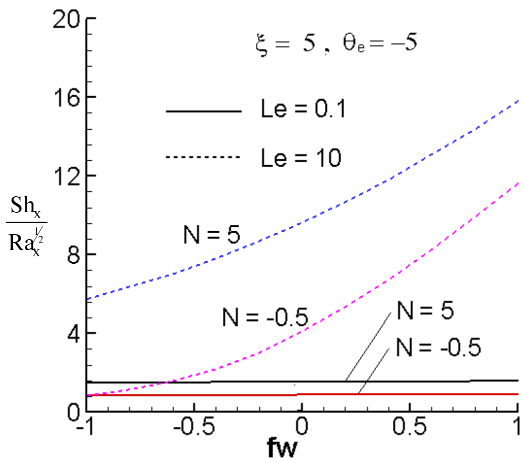

Fig. 11. Effect of the buoyancy ratio and the Lewis number on the local Sherwood number

Figures 12 and 13 illustrate the local Nusselt number $Nu_x / Ra_x^{1/2}$ and the local Sherwood number $Sh_x / Ra_x^{1/2}$ as functions of the blowing/suction parameter f_w for various values of the viscosity-variation parameter with N = 1, Le = 5, ξ = 2, respectively. The red dashed line in Figs. 12 and 13 indicates the case of $\theta_e \to \infty$ (constant viscosity) in comparison with other values of θ_e corresponding to variable viscosity. It is found that for $\theta_e < 0$ (liquid), both the local Nusselt number and the local Sherwood number are greater than the constant viscosity cases, whereas, they are less for $\theta_e > 0$ (gas). This is because for the case of $\theta_e > 0$ (gas) has a tendency to thicken not only the thermal boundary layer thickness but also the concentration boundary layer thickness (δ_T and δ_C), as illustrated in Figs. 6 and 7. The thicker the thermal and concentration boundary layer thicknesses, the smaller the local Nusselt and Sherwood number.

On the other hand, from equation (30), it is also found that for the case of θ_e < 0 (liquid), the effect of viscosity-variation parameter θ_e tends to decrease the viscosity of the fluid μ; consequently accelerating the flow and enhancing the heat transfer rate as well as the mass transfer rate between the surface and the porous medium.

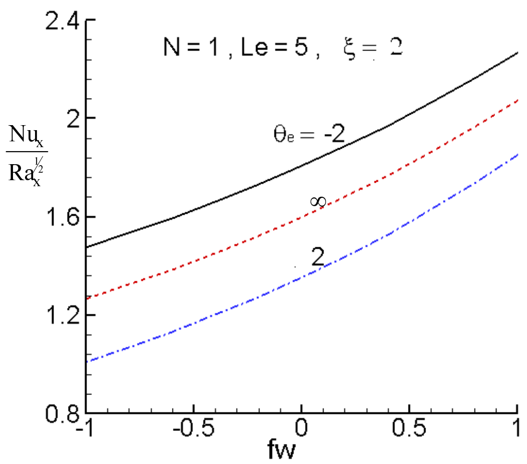

Fig. 12. Effect of the viscosity-variation parameter on the local Nusselt number

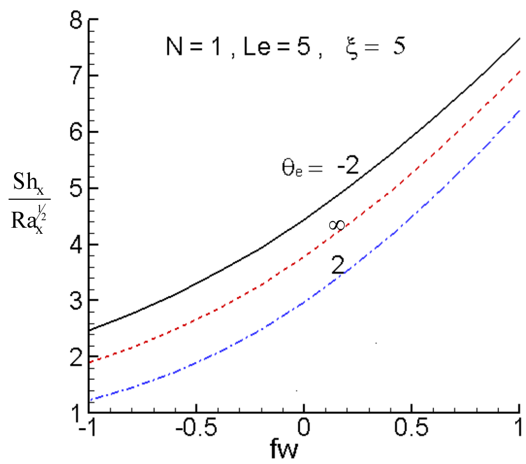

Fig. 13. Effect of the viscosity-variation parameter on the local Sherwood number

The phenomenon of the above results could be also explained with the help of equations (14), (20), and (30). On the one hand, by combining equations (14) and (20), we can rewrite them into the following form:

$$u = \frac{\alpha Ra_x}{x} f' = \frac{\alpha Ra_x}{x}\left(1 - \frac{\theta}{\theta_e}\right)(\theta + N\phi). \qquad (32)$$

For a fixed value of buoyancy value N, for θ_e < 0 (liquid) tends to enhance the Darcy velocity in the x-direction u and accelerate the flow; thus decreasing both the thermal boundary layer thickness and the concentration boundary layer thickness; hence not only increasing the local Nusselt number but also the local Sherwood number.

5. Conclusions

A laminar boundary layer analysis is presented to study the effects of the temperature-dependent viscosity and uniform blowing/suction on natural convection flow in a saturated porous medium resulting from combined heat and mass buoyancy effects adjacent to the vertical cylinder maintained at linear wall temperature and linear wall concentration (LWT/LWC). Numerical solutions are obtained for different values of the viscosity-variation parameter θ_e , the buoyancy ratio N, the Lewis number Le, the transverse curvature parameter ξ, and the blowing/suction parameter f_w . It is shown that for the case of suction (blowing) both the heat and mass transfer rates between the surface and the porous medium increase (decrease). Enhancing the transverse curvature parameter ξ increases the local Nusselt number as well as the local Sherwood number. Increasing the buoyancy ratio N enhances both the local Nusselt number and the local Sherwood number. For a given positive N (negative N), as the Lewis number increases, the local Nusselt number decreases (increases). Whereas, for a given N, as the Lewis number increases, the local Sherwood number always increases. For a porous medium saturated with Newtonian fluids with temperature-dependent viscosity, it is also observed that for the case of $\theta_e < 0$ (liquid) leads to the decrease of the viscosity in fluid flow; thus increasing the local Nusselt number as well as the local Sherwood number (greater than the constant viscosity case). The opposite trend has been observed for the case of $\theta_e > 0$ (gas).

Nomenclature

a	constant
a_1	positive constant
b_1	positive constant
C	concentration
D_M	mass diffusivity
f	dimensionless stream function
f_w	blowing/suction parameter
g	gravitational acceleration
h_x	local convective heat transfer coefficient
$h_{x,m}$	local convective mass transfer coefficient
K	permeability of the porous medium
k	equivalent thermal conductivity
Le	Lewis number
m_w	local mass flux
N	buoyancy ratio
Nu_x	local Nusselt number
p	pressure
q_w	local heat flux
r	transverse coordinate
r_o	radius of the vertical cylinder
Ra_x	modified local Rayleigh number
Sh_x	local Sherwood number
T	temperature
T_e	constant
u	Darcy velocity in the x-direction
v	Darcy velocity in the r-direction
V_w	uniform blowing/suction velocity
x	streamwise coordinate

Greek symbols

α	equivalent thermal diffusivity
β_C	coefficient of concentration expansion
β_T	coefficient of thermal expansion
γ	viscosity-variation constant
δ_C	concentration boundary layer thickness
δ_T	thermal boundary layer thickness
η	similarity variable
θ	dimensionless temperature
θ_e	viscosity-variation parameter
μ	variable viscosity
ξ	transverse curvature parameter
ρ	density
ϕ	dimensionless concentration
ψ	stream function

Subscripts

w	condition at the wall
∞	condition at infinity

References

1. Nield, D. A., and Bejan, A., Convection in Porous Media, 4th Edition, New York,

Springer-Verlag (2013).

2. Vafai, K., Handbook of Porous Media, 2^{nd} Edition, New York, Taylor & Francis (2005).
3. Ingham, D., and Pop, I., Transport Phenomena in Porous Media II, Pergamon, Oxford (2002).
4. Minkowycz, W. J., and Cheng, P., “Free convection about a vertical cylinder embedded in a porous medium,” Int. J. Heat Mass Transfer, Vol. 19, pp. 805-813 (1976).
5. Kumari, M., Pop, I., and Nath, G., “Finite-difference and improved perturbation solution for free convection on a vertical cylinder embedded in a saturated porous medium,” Int. J. Heat Mass Transfer, Vol. 28, pp. 2171-2174 (1985).
6. Merkin, J. H., “Free convection from a vertical cylinder embedded in a saturated porous medium,” Acta Mech., Vol. 62, pp. 19-28 (1986).
7. Bassom, A. P., and Rees, D. A. S., “Free convection from a heated vertical cylinder embedded in a fluid-saturated porous medium,” Acta Mech., Vol. 116, pp. 139-151 (1996).
8. Yücel, A., “The influence of injection or withdrawal of fluid on free convection about a vertical cylinder in a porous medium,” Num. Heat Transfer, Vol. 7, pp. 483-493 (1984).
9. Huang, M. J., and Chen, C. K., “Effects of surface mass transfer on free convection flow over vertical cylinder embedded in a porous medium,” ASME J. Energy Res. Tech., Vol. 107, pp. 394-396 (1985).
10. Lai, F. C., Choi, C. Y., and Kulacki, F. A., “Coupled heat and mass transfer by natural convection from slender bodies of revolution in porous media,” Int. Commun. Heat Mass Transfer, Vol. 17, pp. 609-620 (1990).
11. Yücel, A., “Natural convection heat and mass transfer along a vertical cylinder in a porous medium,” Int. J. Heat Mass Transfer, Vol. 33, pp. 2265-2274 (1990).
12. Singh , B. B., and Chandarki, I. M., “Integral treatment of coupled heat and mass transfer by natural convection from a cylinder in porous media,” Int. Commun. Heat Mass Transfer, Vol. 36, pp. 269-273 (2009).
13. Cheng, C. Y., “Double diffusion from a horizontal cylinder of elliptic cross section with uniform wall heat and mass fluxes in a porous medium”, Int. Commun. Heat Mass Transfer, Vol. 38, pp. 1201-1205 (2011).
14. Gary, J., Kassoy, D. R., Tadjeran, H., and Zebib, A., “The effects of significant viscosity variation on convective heat transfer transport in water-saturated porous medium,” J. Fluid Mech., Vol. 117, pp. 233-249 (1982).
15. Lai, F. C., and Kulacki, F. A., “The effect of variable viscosity on convective heat transfer along a vertical surface in a saturated porous medium,” Int. J. Heat Mass Transfer, Vol. 33, pp. 1028-1031 (1990).
16. Kumari, M., “Variable viscosity effects on free and mixed convection boundary-layer flow from a horizontal surface in a saturated porous medium- variable heat flux,” Mech. Res. Commun., Vol. 28, pp. 339-348 (2001).
17. Vajravelu, K., Prasad, K. V., Gorder, R. A. V., and Lee J., “Free convection boundary layer flow past a vertical surface in a porous medium with temperature-dependent properties,” Trans. Porous Media, vol. 90, pp. 977-992, 2011.
18. Cheng, C. Y., “Nonsimilar boundary layer analysis of double-diffusive convection from

a vertical truncated cone in a porous medium with variable viscosity," Appl. Math. Comp., Vol. 212, pp. 185-193 (2009).

19. Mahdy, A., "Effect of chemical reaction and heat generation or absorption on double-diffusive convection from a vertical truncated cone in porous media with variable viscosity," Int. Commun. Heat Mass Transfer, Vol. 37, pp. 548-554 (2010).
20. Mahdy, A., Chamkha, A. J., and Baba, Y., "Double-diffusive convection with variable viscosity from a vertical truncated cone in porous media in the presence of magnetic field and radiation effects," Comp. Math. Appl., Vol. 59, pp. 3867-3878 (2010).
21. Hassanien, I. A., and Rashed, Z. Z., "Non-Darcy free convection flow over a horizontal cylinder in a saturated porous medium with variable viscosity, thermal conductivity and mass diffusivity," Commun. Nonlinear Sci. Numer. Simulat., Vol. 16, pp. 1931-1941 (2011).
22. Hong, J. T., Yamada, Y., and Tien, C. L., "The effects of non-Darcian and non-uniform porosity on vertical plate- natural convection in porous media," J. Heat Transfer, Vol. 109, pp. 356-362 (1987).
23. Yih, K. A., "Coupled heat and mass transfer by free convection over a truncated cone in porous media: VWT/VWC or VHF/VMF," Acta Mech., Vol. 137, pp. 83-97 (1999).
24. Cebeci, T., and Bradshaw, P., Physical and Computational Aspects of Convective Heat Transfer, New York, Springer-Verlag (1984).